

https://dspace.org/

Elastic properties of glasses and glass ceramics at high pressures and high temperatures

Gravett, Salome

2015-01-22
http://hdl.handle.net/10539/16700

Downloaded from a DSpace repository. https://dspace.org/

Expanding equation (2.13a) gives

$$S_1 = s_{11}T_1+s_{12}T_2+s_{13}T_3+s_{14}T_4+s_{15}T_5+s_{16}T_6$$
$$(i = 1;\ j = 1, 2,\ldots \text{ or } 6) \qquad (2.24)$$

Now, if the only stress acting is T_1 then all six strains S_1, S_2,... and S_6 exist. In the case of S_1 equation (2.24) gives

$$S_1 = s_{11}T_1 \text{ and therefore } s_{11} = 1/E_1, \qquad (2.25)$$

where E_1 is the Young's modulus in the x_1 direction. If the only stress is T_2,

$$S_1 = s_{12}T_2$$

But $S_1/S_2 = -\sigma_{21}$, where σ_{21} is the Poisson's ratio and $S_2 = s_{22}T_2$ (see equation (2.25)). Therefore

$$s_{12} = -\sigma_{21}/E_2,$$

and since $s_{12} = s_{21}$ (section 2.2.2),

$$s_{12} = -\sigma_{21}/E_2 = -\sigma_{12}/E_1$$

Then equation (2.22) for isotropic materials becomes

$$K = 1/B = 3(1-2\sigma)/E$$
$$\text{and } B = E/(3(1-2\sigma)) \qquad (2.26)$$

which is a relation, additional to equation (2.16), between the elastic parameters of isotropic materials. The full set of relations between elastic parameters of isotropic bodies is summarized in Table 2.1 for completeness.

d) Using the information of Table 2.1 (Schreiber, et al., 1973) the following equations can be used to calculate σ and E from L and G.

$$\sigma = (\rho(v_\ell^2 - 2v_s^2))/(2\rho(v_\ell^2 - v_s^2))$$
$$= (L - 2G)/2(L - G) \qquad (2.27)$$

$$E = 2G(1 + \sigma)$$
$$2G + (2LG - 4G^2)/(2(L-G))$$
$$= (4LG - 4G^2 + 2LG - 4G^2)/(2(L-G))$$
$$= (3LG - 4G^2)/(L - G) \qquad (2.28)$$

Table 2.1: The connection between elastic constants of isotropic bodies (Adapted from Schreiber, et al., 1973)

B	E	$\lambda\ (C_{12})$	σ	$L = \rho v_l^2$	$G = \rho v_s^2$	How obtained
$\lambda + \frac{2G}{3}$	$G\frac{3\lambda + 2G}{\lambda + G}$	.....	$\frac{\lambda}{2(\lambda + G)}$	$\lambda + 2G$	.....	λ is always calculated
.....	$9B\frac{B - \lambda}{3B - \lambda}$	.....	$\frac{\lambda}{3B - \lambda}$	$3B - 2\lambda$	$\frac{3(B - \lambda)}{2}$	λ is always calculated
.....	$\frac{9BG}{3B + G}$	$B - \frac{2G}{3}$	$\frac{3B - 2G}{2(3B + G)}$	$B + \frac{4G}{3}$	.....	Static measurement of B and G
$\frac{EG}{3(3G - E)}$	.....	$G\frac{E - 2G}{3G - E}$	$\frac{E}{2G} - 1$	$G\frac{4G - E}{3G - E}$	.....	Static measurement of E and G; dynamic (resonance) measurement of E and G
.....	.....	$3B\frac{3B - E}{9B - E}$	$\frac{3B - E}{6B}$	$3B\frac{3B + E}{9B - E}$	$\frac{3BE}{9B - E}$	Static measurement of B; dynamic (resonance) measurement of E
$\lambda\frac{(1 + \sigma)}{3\sigma}$	$\lambda\frac{(1 + \sigma)(1 - 2\sigma)}{\sigma}$	.....	.....	$\lambda\frac{(1 - \sigma)}{\sigma}$	$\lambda\frac{1 - 2\sigma}{2\sigma}$	
$G\frac{2(1 + \sigma)}{3(1 - 2\sigma)}$	$2G(1 + \sigma)$	$G\frac{2\sigma}{1 - 2\sigma}$	.....	$G\frac{2 - 2\sigma}{1 - 2\sigma}$	.....	Static or dynamic measurement of G and σ (e.g., using sphere resonance)
.....	$3B(1 - 2\sigma)$	$3B\frac{\sigma}{1 + \sigma}$	.....	$3B\frac{1 - \sigma}{1 + \sigma}$	$3B\frac{1 - 2\sigma}{2 + 2\sigma}$	Static measurement of B and σ
$\frac{E}{3(1 - 2\sigma)}$	.....	$\frac{E}{(1 + \sigma)(1 - 2\sigma)}$	.....	$\frac{E(1 - \sigma)}{(1 + \sigma)(1 - 2\sigma)}$	$\frac{E}{2 + 2\sigma}$	Static or dynamic measurement of E and σ
$\rho(v_l^2 - \frac{4}{3}v_s^2)$	$\frac{3v_s^2v_l^2 - \frac{4}{3}v_s^4}{(v_l^2 - v_s^2)}$	$\rho(v_l^2 - 2v_s^2)$	$\frac{v_l^2 - 2v_s^2}{2(v_l^2 - v_s^2)}$	.....	.....	Dynamic (velocity) measurement of v_l and v_s

Ledbetter (1983) provided a useful summary of the various elastic constants in the following way:

a) Young's modulus, E

This is the most familiar elastic constant, as evidenced by the many ways in which it is described: extension modulus, tensile modulus, tension modulus, elastic modulus and modulus. E is related to the extensional sound wave velocity, v_e, in a rod by

$$v_e = (E/\rho)^{\frac{1}{2}} \qquad (2.29)$$

b) Shear modulus, G

Shear as well as torsion conserve volume but change shape, where the bulk modulus describes volume change without shape change. G determines the velocity of a shear-polarized or transverse sound wave (v_s or v_t) in a plate or of a torsional wave in a rod according to

$$v_{s,t} = (G/\rho)^{\frac{1}{2}} \qquad (2.30)$$

c) Compressibility, K

All matter - gas, liquid or solid - responds to pressure change and exhibits at least one elastic constant, the compressibility, where

$$K_T = -(1/V)(\partial V/\partial P)_T \qquad (2.31)$$

d) Bulk modulus, B

Scientists often use B to describe a solid's resistance to volume change, rather than compressibility. For isotropic materials, B and K relate reciprocally:

$$B_T = 1/K_T = -V(\partial P/\partial V)_T \qquad (2.32)$$

e) Poisson's ratio, σ

σ is not an elastic modulus, but a dimensionless ratio of two elastic compliances. Usually defined by a uniaxially stressed rod (E) experiment, σ is the negative ratio of transverse (s) and longitudinal

(ℓ) strains,

$$\sigma = -\epsilon_s/\epsilon_\ell \qquad (2.33)$$

Theoretically, σ is bounded by -1 and ½, but negative σ values are never observed in quasi-isotropic materials. Thus, in polycrystals σ is bounded practically by 0 and ½. A typical value for metals is 1/3. Between 0.28 and 0.42 being the observed range for most materials. Such σ values mean that a material tends to maintain constant volume during uniaxial deformation. If σ is ½ no volume change occurs during deformation.

2.3 Elastic constants of glasses and glass ceramics with pressure and temperature

Glass is described as a non-crystalline material that has no regular internal structure. It is rigid at ordinary temperatures and soft or almost fluid at high temperatures. As a glass-forming liquid is cooled some of its properties change sharply in a narrow temperature range (Doremus, op. cit.). Other properties, such as the heat capacity and electrical conductivity also change abruptly at about the same temperature, called the glass transition temperature.

The expectation is that elastic moduli would decrease with increasing temperature for any material according to the character of interatomic forces. Metals and ceramics do usually show this behaviour, but fused silica does not. Sosman (1927) recorded that the torsional modulus of fused silica increases with temperature at the rate of about 0.012 %/°C. The free-volume concept explains this: bonds deformed in flexure would be expected to vibrate in a strongly anharmonic manner that will tend to restore the mean bond angle to its undistorted value.

As far as their elastic behaviour depends upon temperature and hydrostatic pressure glasses divide into two different kinds (El-Mallawany and Saunders, 1987):

a) Vitreous silica and silica-based glasses which have anomalously negative pressure derivatives and positive temperature dependences of the bulk and the shear moduli.

b) Most other glasses behave more normally in that the pressure

derivatives of the bulk and shear moduli are positive and their temperature derivatives are negative.

Manghnani (1970) investigated 125 glasses of diversified composition under atmospheric conditions as well as under pressures up to 0.7 GPa, and to temperatures of 400 °C. The types of glasses investigated were vitreous silica, silicate and borosilicate glasses, and calcium aluminate and other high modulus glasses. He found that the SiO_2 content is the most important factor determining the properties of the silicate glasses. The above-mentioned anomalous behaviour, under pressures and temperatures, if present, can be quantatively related to the SiO_2 content. Within one system, e.g., Na_2O-TiO_2-SiO_2, the elastic properties of the glasses vary systematically with composition and specifically with the SiO_2/Na_2O ratio. Manghnani also did infrared absorption studies on a few of these glasses up to 5.88 GPa.

All the vibrational frequencies in α-quartz increased with pressure, whereas the Si-O-Si frequency in fused silica, Vycor and Pyrex glasses decreased with pressure, reflecting an increase in the bond angle and decreasing elastic parameters with pressure. He concluded that the disordered structure of glass tends to become ordered under high pressures. Further discussion on the infrared absorption technique is beyond the scope of this study.

Measurements of the second-order adiabatic elastic moduli and pressure and temperature derivatives of a sodium silicate and a sodium alumino-silicate glass showed increasing longitudinal and decreasing shear wave velocities with pressure (El-Mallawany and Saunders, op. cit.). These two glasses have almost the same oxygen packing densities and unoccupied volumes. On comparing the two glasses it becomes clear that the elastic moduli increase substantially with substitution of aluminum for silicon.

Increases in the shear modulus are a result of the elimination of non-bonding oxygen atoms. On the other hand, changes in the bulk and Young's moduli are associated with bond strengths in the tetrahedra network or with steric hindrance effects. However aluminum

derivatives of the bulk and shear moduli are positive and their temperature derivatives are negative.

Manghnani (1970) investigated 125 glasses of diversified composition under atmospheric conditions as well as under pressures up to 0.7 GPa, and to temperatures of 400 °C. The types of glasses investigated were vitreous silica, silicate and borosilicate glasses, and calcium aluminate and other high modulus glasses. He found that the SiO_2 content is the most important factor determining the properties of the silicate glasses. The above-mentioned anomalous behaviour, under pressures and temperatures, if present, can be quantatively related to the SiO_2 content. Within one system, e.g., Na_2O-TiO_2-SiO_2, the elastic properties of the glasses vary systematically with composition and specifically with the SiO_2/Na_2O ratio. Manghnani also did infrared absorption studies on a few of these glasses up to 5.88 GPa.

All the vibrational frequencies in α-quartz increased with pressure, whereas the Si-O-Si frequency in fused silica, Vycor and Pyrex glasses decreased with pressure, reflecting an increase in the bond angle and decreasing elastic parameters with pressure. He concluded that the disordered structure of glass tends to become ordered under high pressures. Further discussion on the infrared absorption technique is beyond the scope of this study.

Measurements of the second-order adiabatic elastic moduli and pressure and temperature derivatives of a sodium silicate and a sodium alumino-silicate glass showed increasing longitudinal and decreasing shear wave velocities with pressure (El-Mallawany and Saunders, op. cit.). These two glasses have almost the same oxygen packing densities and unoccupied volumes. On comparing the two glasses it becomes clear that the elastic moduli increase substantially with substitution of aluminum for silicon.

Increases in the shear modulus are a result of the elimination of non-bonding oxygen atoms. On the other hand, changes in the bulk and Young's moduli are associated with bond strengths in the tetrahedra network or with steric hindrance effects. However aluminum

substitution does not affect the pressure derivatives of the moduli. These derivatives are proportional to the unoccupied volume fraction in the glass, and this is a measure of ion packing efficiency. The conclusion is then that only packing efficiency controls pressure derivatives in alumino-silicate glasses and that the thermal properties are associated with motion of bridging oxygen atoms.

Glass ceramics are polycrystalline solids made by the controlled crystallization of glass (Hlavac, 1983). The manufacturing process entails:

a) melting and forming of the products by glass-working processes;
b) heat treatment to convert the product to a final crystalline one.

Crystallization takes place throughout the entire glass volume in the presence of substances which accelerate the nucleation. Such a product has a uniform and fine-grained structure. The normal crystal size is 0.1 to 1 μm.

This is a particularly advantageous process in that the new product has various specific properties: the homogeneous glass has a uniform ceramic-like structure which has a considerably higher strength than that of the original glass. It also has a very low or even zero thermal expansion. Other advantages are:

a) The possibility of continuously changing the properties only by adjusting the initial glass composition and eventually also the final phase composition;
b) The higher efficiency of glass-working processes especially with products which are difficult to shape; etc.

It is important to bear in mind that although the properties of a glass or glass ceramic are a function of composition, other factors can often have important effects on observed properties (Handbook of Materials Science, 1975). Such factors include atmospheric weathering, which can modify the materials' surface chemistry behaviour, and thermal history which can alter molecular structure and phase constitution.

The moduli of elasticity for glass ceramics are higher than those of

ordinary glasses and of some conventional ceramics, and they are lower than those of sintered pure oxide ceramics (McMillan, 1979). For glasses, Young's modulus can be calculated from the chemical glass composition by using factors which have been derived for this purpose because it seems as if Young's modulus is an additive function of chemical composition. Freiman and Hench (1972) confirmed that the modulus of elasticity of a polyphase ceramic will also have an additive relationship with the individual characteristics of the crystalline and glassy phases.

It is expected that the value of the Young's modulus in a glass ceramic is primarily dependent on the elastic constants of the major crystalline phases. However, the presence of oxides in the glass phase promotes high values of Young's modulus and therefore must also be brought into account. Oxides which have a marked influence upon the elastic moduli of glasses, are particularly, calcium oxide, magnesium oxide and aluminium oxide.

It is not possible to form a complete idea of the relationship between microstructure and elastic properties without knowledge of the volume fractions of the various crystal and residual glass phases. Another approach would be to consider the influence of systematic variations of the composition and microstructure.

Varying the heat-treatment schedule of a glass ceramic permits development of different volume fractions of crystal phases. The influence upon elastic properties can then be examined.

When the volume fraction of a crystalline phase is low, $< 0.35 - 0.4$, the glass forms an almost continuous matrix with isolated crystals. In such a case it is expected that the properties of the glass ceramic would be influenced by the properties of the vitreous phase. In the case where the volume fractions of the two phases are almost equal, they tend to form interpenetrating networks. Where the volume fraction of the crystalline phase is high, the glass forms a thin layer between crystals or forms isolated pockets at the grain boundaries (McMillan, op. cit.).

2.4 Measurement of elastic constants

The measurement of ultrasonic wave velocities is an accurate way of determining elastic constants (Crecraft, 1983). Ultrasonic waves are stress waves at frequencies above the audible range. In gases and liquids, which can support only hydrostatic stress, ultrasonic waves are basically similar to audible sound waves in air, with the particle motion in the direction of wave propagation. These waves are called longitudinal or compressional. In the case of solids which can support uniaxial stress as well as shear stress, both longitudinal and shear waves can be propagated.

When the relations shown in equation (2.9) are transformed to the Voigt notation and substituted into equation (2.13b) for the cubic system, it follows:

$$\begin{aligned} T_1 &= (C_{11}-C_{12})\partial u/\partial x + C_{12}(\partial u/\partial x+\partial v/\partial y+\partial w/\partial z) \\ T_2 &= (C_{11}-C_{12})\partial v/\partial y + C_{12}(\partial u/\partial x+\partial v/\partial y+\partial w/\partial z) \\ T_3 &= (C_{11}-C_{12})\partial w/\partial z + C_{12}(\partial u/\partial x+\partial v/\partial y+\partial w/\partial z) \\ T_4 &= C_{44}(\partial v/\partial z+\partial w/\partial y) \\ T_5 &= C_{44}(\partial u/\partial z+\partial w/\partial x) \\ T_6 &= C_{44}(\partial u/\partial y+\partial v/\partial x) \end{aligned} \qquad (2.34)$$

For an ultrasonic wave propagating in the x direction the equation of motion is

$$\rho(\partial^2 u/\partial t^2) = \partial T_1/\partial x + \partial T_6/\partial y + \partial T_5/\partial z \qquad (2.35)$$

where u is the displacement in the x direction as before. Similar equations hold for the y and z directions. Substitution of equations (2.34) into (2.35) gives the wave equation for crystals of cubic symmetry:

$$\begin{aligned} \rho(\partial^2 u/\partial t^2) &= (C_{11}-C_{12})\partial^2 u/\partial x^2 \\ &+C_{12}(\partial^2 u/\partial x^2+\partial^2 v/\partial x\partial y+\partial^2 w/\partial x\partial y) \\ &+C_{44}(\partial^2 u/\partial y^2+\partial^2 u/\partial z^2+\partial^2 v/\partial x\partial y+\partial^2 w/\partial x\partial y) \end{aligned} \qquad (2.36)$$

with similar equations for the y and z directions. These equations are solved by substituting into (2.36) the relations for a plane wave,

namely

$$u = A_1 \exp 2\pi i(\omega t - k_1 x - k_2 y - k_3 z)$$
$$v = A_2 \exp 2\pi i(\omega t - k_1 x - k_2 y - k_3 z) \qquad (2.37)$$
$$w = A_3 \exp 2\pi i(\omega t - k_1 x - k_2 y - k_3 z)$$

where ω is the wave frequency and k_i is related to the wave number.

The result of this substitution is three simultaneous homogeneous equations in A_1, A_2 and A_3:

$$[(C_{11}-C_{14})k_1^2+C_{44}k^2-\rho\omega^2]A_1+(C_{12}+C_{44})k_1k_2A_2$$
$$+(C_{12}+C_{44})k_1k_3A_3 = 0$$

$$(C_{12}+C_{44})k_1k_2A_1+[(C_{11}-C_{44})k_2^2-\rho\omega^2]A_2 \qquad (2.38)$$
$$+(C_{12}+C_{44})k_2k_3A_3 = 0$$

$$(C_{12}+C_{44})k_1k_3A_1+(C_{12}+C_{44})k_2k_3A_2$$
$$+[(C_{11}-C_{44})k_3^2+C_{44}k^2-\rho\omega^2]A_3 = 0$$

The determinant of the coefficients must vanish in order that not all components of amplitude are zero. The phase velocity, v, yields the appropriate elastic modulus M of the mode being propagated by the relationship:

$$v = (M/\rho)^{\frac{1}{2}}$$

Simple expressions can be obtained relating the elastic constants to the ultrasonic velocity and density, where the elastic parameter M of the above equation is in general a linear combination of one or more elastic stiffnesses (constants). The velocity is simply $v=\omega/k$, since dispersion is absent for sufficient long waves. Substitution of the values of k and A into equations (2.38) yields the following simple expressions: In the x direction, $k_1 = k$, $k_2 = k_3 = 0$. In this case, the particle motion of a longitudinal wave is also in the x direction, so that $A_1 = A$, $A_2 = A_3 = 0$ describes the longitudinal wave. The longitudinal velocity, v_ℓ, is given by the relation

$$\rho v_\ell^2 = C_{11} \qquad (2.39)$$

The velocity v_t of plane transverse waves, polarized in any direction perpendicular to the x axis, is given by

$$\rho v_t^2 = C_{44} \qquad (2.40)$$

Many physical phenomena influence the moduli of materials and the attenuation coefficients for various modes, and this can be investigated by measuring the ultrasonic wave velocities and the attenuation, respectively. Therefore in this study ultrasonic wave velocities have been measured.

3. EXPERIMENTAL TECHNIQUE

3.1 Elasticity and its measurement at high pressure and high temperature

3.1.1 Review of elasticity measurements

Although elastic constants are measured by a great variety of methods, there are only four principal approaches:

a) Static stress-strain: These methods impose a stress and measure a strain response. The stress-strain ratio is then the elastic constant.

b) Subresonant forced vibration: These methods are used at very low frequencies up to 100 Hz. At low stress levels of about 0.1 MPa, the ratio of the stress-strain amplitude is determined. Damping can then by measured as the phase lag of the strain wave behind the stress wave or determined by examining the logarithmic decay of the stress wave after it is switched off.

c) Resonance: Resonance methods establish standing waves by varying the stress frequency. Then use the classical vibration theory to determine elastic constants using mass density, geometry of the specimen and the resonance frequency. A typical specimen is a few centimetres in the largest dimension; normally one-half wavelength. Resonance frequencies are usually between 10 and 100 kHz while the peak stress is 0.1 MPa or lower. In this case damping is established from the halfwidth of the amplitude vs frequency graph.

d) Pulse: These methods make use of travelling acoustic waves with short wavelengths compared to the specimen size (about 1 cm). Elastic constants are determined from the velocity of a sound wave through a specimen of a certain length. This velocity is derived from the pulse

transit time through this specimen. Frequencies are normally about 10 MHz and the peak stress is 10 kPa or lower.

Pulse experiments determine the C_{ij}'s directly while resonance and static stress-strain experiments determine the s_{ij}'s directly.

Other methods for measuring elastic constants include static deformation, Brillouin scattering, diffuse X-ray reflection and neutron scattering. The accuracy of these methods varies widely.

3.1.2 The pulse echo overlap method

a) General: The pulse echo overlap (PEO) method is a highly accurate method for measuring the velocity of ultrasonic waves in materials. This fact will be illustrated later on.

The PEO method has four features that other methods usually do not possess simultaneously (Papadakis, 1976):

i) This method can be used with the transducer bonded directly to the specimen or with a buffer rod between the transducer and the specimen. This feature was very useful in the experimental design of this study.

ii) This method may be operated with both broadband pulses or radio frequency (r.f.) signals.

iii) The method can be used to make through-transmission measurements of the travel time on a single pass between two transducers.

iv) The method can be adapted to measure both group velocity and phase velocity.

On the other hand, the PEO method probably cannot be automated, because the echoes are overlapped by the observer in oscilloscope time.

b) Velocity measurement: In this study, the specimen dimensions are limited by the size of the pressure cell and are typically about 10 mm in diameter and 10 mm in length. The mathematical theory for wave propagation in solids deals with an infinite medium and consequently to apply it to a finite medium such as this specific sample, an ultrasonic wave with wavelength small in comparison to the specimen dimensions should be propagated. This requirement is satisfied by using a frequency in the region of 10 MHz, since below about 1 MHz the mathematical theory no longer applies, and above 20 MHz the acoustic surface impedance limits the ability to transmit and receive the energy. With increasing frequency an increase in attenuation is experienced, thus also limiting the frequency range to work in.

Figure 3.1 shows a diagram of the essential components of the pulse echo overlap system. Ultrasonic vibrational pulses from a piezoelectric transducer (usually quartz) are introduced into the sample. A small amount of bonding agent is used between the sample and the transducer to enhance transmission of the waves between the sample and transducer. The R.F. Unit generates a continuous radio frequency signal which is used to excite the transducer. The transducers are X- and Y-cut crystalline quartz, cut to a particular dimension so that their resonant frequency is 10 MHz. They are gold-sputtered to provide electrode contacts on the opposite surfaces of the crystal. The longitudinal and shear waves are generated by the X- and the Y-cut transducers respectively.

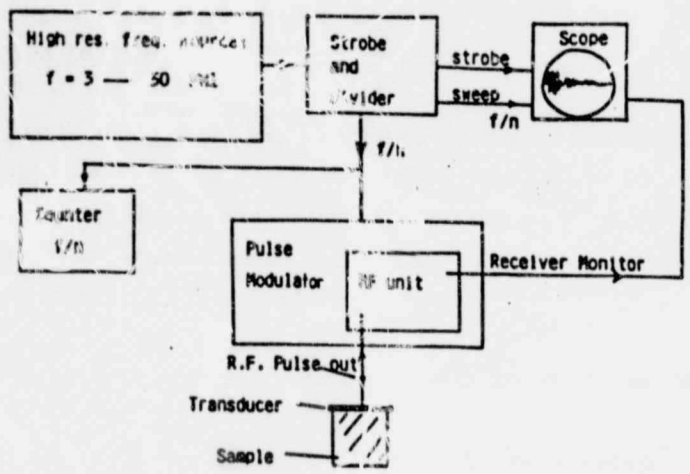


Fig. 3.1 The essential components of the pulse echo overlap system

The input is required to be pulsed rather than continuous, therefore the "Pulse Modulator" unit is used to modulate the radio frequency signal. The basis of this method is to send a pulse into the cylindrical sample and examine the echoes obtained. If the opposite faces of the sample are flat and parallel the signal will b reflected from the opposite face and return to the same transducer having suffered only attenuation. However, a certain amount of dispersion is to be expected and due to the finite sample dimensions a measure of interference as well. The echo is detected by the transducer and repeated reflections cause a series of diminishing echoes (Figure 3.2(a)) as displayed on the oscilloscope screen.

If a buffer rod of sufficient length is used between the transducer and the specimen, the pulse sent by the transducer can be reflected several times within the specimen, and several of them can return back to the transducer, before any multiple echoes in the buffer rod have returned back to the transducer. This echo train is shown in figure 3.2(b)

To determine the velocity of a wave two echoes are examined on the oscilloscope screen. For example, if the first and second echoes are chosen then the time difference between them is the time taken for the signal to travel across the sample, reflects and returns to the transducer. This means that if the sample is of length ℓ, the signal travels a distance of 2ℓ in the time period separating the two echoes. The introduction of a delay into the second signal allows the two signals to be superimposed on the screen (Figure 3.2(c)). The first signal is used to trigger the x-axis sweep.

Fine adjustment of the driving frequency enables accurate overlapping of the signals, r.f. cycle for r.f. cycle within the echo and hence an accurate value for their time separation, 1/f. The frequency f kHz is displayed on the counter and has to be converted into an elastic modulus. Equations (2.39) and (2.40) give

$$M = \rho v^2 \qquad (3.1)$$

ρ is measured using Archimedes' principle with water as the immersant.

Since the time taken to travel a distance 2ℓ is measured, it follows

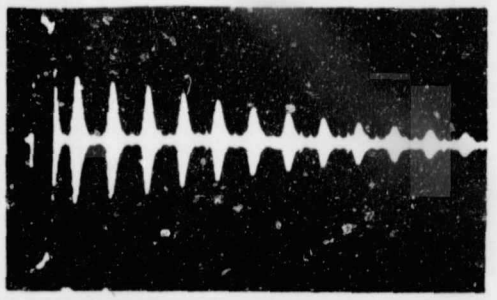


Fig. 3.2(a) A series of diminishing echoes after Schreiber et al., 1973)

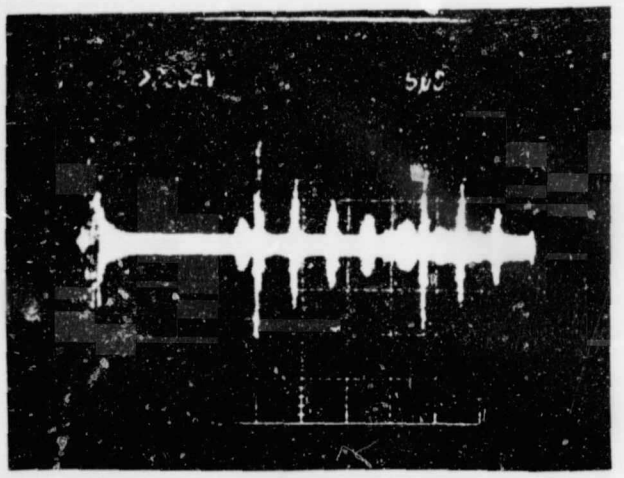


Fig. 3.2(b) The echo train obtained when using a buffer rod (after Levitt, 1987)

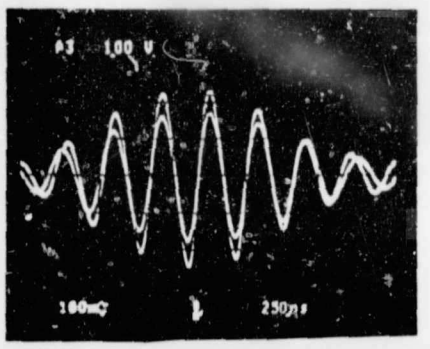


Fig. 3.2(c) Two echoes being overlapped (after Grigg et al., 1986)

that

$$M = \rho(2\ell f,^2 = 4\rho\ell^2 f^2 \qquad (3.2)$$

The question can now arise: "Which cycle of the first echo corresponds to which cycle of the next echo?" There is an unambiguous way to pick the true cycle-for-cycle overlap for r.f. signals in nondispersive media. This is to use the McSkimin Δt criterion (McSkimin, 1961; McSkimin and Andreatch, 1962). This method is being used only in more complex measurements and it was not necessary to be used here.

In the present work the first two consecutive echoes were always overlapped and tuning has been verified by measuring sample velocity with a broad-band pulse to obtain the correct overlap frequency prior to use.

c) The MATEC system: For this study the MATEC system was used with the PEO method. The components used in the present set-up are shown in figure 3.3 and include the following:

a) MATEC pulse modulator and receiver; model 6600
b) MATEC high resolution frequency source; model 110
c) MATEC decade dividers and dual delay generators; model 122B
d) MATEC 100 MHz filter
e) MATEC 50 MHz filter
f) MATEC r.f. plug-in; model 760 V
g) MATEC impedance matching network; model 70
h) Hewlett Packard universal counter; model 5314A
i) Tektronix Oscilloscope; model 7613

The "High Resolution Frequency Source" (HRFS) is capable of producing a finely variable frequency in the range of 0.3 Hz to 53 MHz. This frequency is produced as a continuous wave and is used in two ways. Firstly to produce the overlap frequency from the strobe and divider box, that drives the x-axis sweep. A typical overlap frequency is in the range 30 to 500 kHz and therefore the overlap frequency needs to be divided down to that band. Secondly, to enable continuous viewing on the screen, the pulses must be repeatedly sent in. Consecutive pulses

Author Gravett Salome
Name of thesis Elastic Properties Of Glasses And Glass Ceramics At High Pressures And High Temperatures. 1989

PUBLISHER:
University of the Witwatersrand, Johannesburg
©2013

LEGAL NOTICES:

Copyright Notice: All materials on the University of the Witwatersrand, Johannesburg Library website are protected by South African copyright law and may not be distributed, transmitted, displayed, or otherwise published in any format, without the prior written permission of the copyright owner.

Disclaimer and Terms of Use: Provided that you maintain all copyright and other notices contained therein, you may download material (one machine readable copy and one print copy per page) for your personal and/or educational non-commercial use only.

The University of the Witwatersrand, Johannesburg, is not responsible for any errors or omissions and excludes any and all liability for any errors in or omissions from the information on the Library website.